

# Randomized Kaczmarz Algorithm Applied D'Hondt Method for Extremely Massive MIMO Wireless Communication Systems

TATSUKI FUKUDA,  
Department of Data Science, Faculty of Data Science,  
Shimonoseki City University,  
2-1-1 Daigakucho, Shimonoseki City, Yamaguchi, 751-8510,  
JAPAN

*Abstract:* - Extremely massive MIMO (Multiple-Input Multiple-Output) is a technique to enable the spatial diversity. The systems employ a large number of antennas at the base stations, resulting in high computational complexity in various processes of wireless communications. The precoding process is one of them because the process requires the calculation of matrix inversion. The randomized Kaczmarz algorithm (rKA) is an iterative method to obtain the approximation so the computational time of precoding can be decreased. Some improvements of rKA were proposed so far, the iteration number required to obtain the approximation of inverse matrix is not so small. In this paper, we propose a new rKA method that applies the D'Hondt method, typically used for seat allocation in elections. In rKA process, the row vector is selected to use for updating approximation. Our method selects the row vector based on the D'Hondt method while the conventional rKA methods select the row vector probabilistic. Some results of simulation showed that the bit error ratio (BER) performance of our method is superior to other rKA methods at higher normalized transmit powers (NTP). The results also showed that the BER performances of our method with small number of iterations are more accurate than the others especially at high NTPs. That means our method can achieve the same BER performance with smaller number of iterations as the others, so the computational complexity of precoding with rKA is decreased.

*Key-Words:* - Massive MIMO, Precoding, rKA, RZF, D'Hondt method.

Received: March 2, 2024. Revised: September 3, 2024. Accepted: October 3, 2024. Published: November 15, 2024.

## 1 Introduction

The COVID-19 pandemic, which began around 2020, has led to a rapid advancement in the online transformation of societal infrastructure. The increasing network traffic has further escalated due to the explosive growth in the user base of various services, such as video streaming platforms, and the widespread use of online tools for work and education. Wireless connectivity is now more prevalent than ever, with devices such as smartphones and Internet-of-Things (IoT) devices, [1], [2], [3], [4], requiring reliable connections.

To meet the demands of this immense network traffic, high-speed and stable wireless communication is critical. Technologies like Multiple-Input Multiple-Output (MIMO), which enable the use of multiple antennas to transmit multiple signals simultaneously, have been key to achieving this. MIMO systems have become a cornerstone of 5G networks, providing improved spectral efficiency and system capacity.

As we transition towards 6G, the next generation of wireless communication systems, even more advanced techniques are needed to handle the growing data demands.

Extremely massive MIMO, [5], an extension of conventional MIMO, involves the deployment of

hundreds or even thousands of antennas at base stations, allowing for enhanced spatial diversity and beamforming capabilities. This technique promises to further increase spectral and energy efficiency, [6], making it a crucial technology for 6G systems. However, the computational complexity of processes such as precoding also grows significantly as the number of antennas increases, [7], [8], [9], [10], [11], [12], [13].

The linear tensor zero-forcing (ZF) method, [14], is a widely used technique for signal detection in receivers and precoding in transmitters. However, while ZF can effectively eliminate inter-user interference, its bit error ratio (BER) characteristics are often not practical in large-scale systems due to its sensitivity to noise. To address this, improved methods such as the regularized ZF (RZF) method, [15], have been proposed, but the matrix inversion required by these methods becomes a major bottleneck in extremely massive MIMO systems.

To reduce this complexity, iterative methods like the randomized Kaczmarz algorithm (rKA) have been proposed, [16]. rKA approximates the solution to the large linear systems involved in precoding, without the need for direct matrix inversion. However, while

rKA reduces computational cost, the number of iterations required for convergence is still a challenge. Several improved variants of rKA have been developed, [17], but they still face limitations, especially in extremely massive MIMO systems. Most conventional methods for precoding, such as those used in uplink scenarios, [18], [19], [20], assume that the channel is stationary, [21]. However, in extremely massive MIMO systems, the long antenna arrays lead to non-stationary channel conditions, where the channel varies significantly over different antennas, [22]. This study focuses on precoding in the downlink environment, where non-stationary channels pose a significant challenge.

In this paper, we propose a novel approach that applies the D'Hondt method, typically used for seat allocation in elections, to the randomized Kaczmarz algorithm for precoding in extremely massive MIMO systems. By improving the selection process of row vectors during iterations, our method achieves faster convergence and better BER performance, particularly at higher normalized transmit powers (NTP). This contribution reduces the computational complexity of precoding and demonstrates superior performance compared to other existing rKA-based methods.

Organization: The rest of this paper is organized as follows. In Section II, the preliminary knowledges including the model assumed in this study are explained. In Section III, the Kaczmarz Algorithm and improved methods of it are shown for precoding process. Our proposed method is also described in the section. In Section IV, the BER performances of the methods are shown used results of some computer simulations. The conclusions are drawn in Section V.

## 2 Preliminaries

First, let us provide a summary of the fundamental aspects relevant to this study.

### 2.1 Model

We establish the framework for the Massive MIMO wireless communication system investigated in this study. Initially, the base station is equipped with  $M$  antennas, catering to  $K$  user devices, with each device having a single antenna. The  $M$  antennas at the base station are partitioned into  $S$  subarrays, where the  $s$ -th subarray comprises  $M_s$  antennas, and each subarray accommodates a distributed set of user devices. The number of user devices connected to subarray  $j$  is denoted as  $K_j$ , as expressed in (1).

$$K = \sum_j K_j. \quad (1)$$

In this context, let us denote  $y_{j,k}$  as the received signal by the  $k$ -th user device  $U_{j,k}$  connected to the

$j$ -th subarray. The transmitted signal from the  $s$ -th subarray is represented by  $\mathbf{x}_s$ , while  $\mathbf{h}_{j,k}^s$  signifies the channel vector between the  $s$ -th subarray and  $U_{j,k}$ . The channel matrix between the  $s$ -th subarray in the base station and  $K_j$  user devices in the  $j$ -th subarray is denoted as  $\mathbf{H}_j^s = [\mathbf{h}_{j,1}^s, \mathbf{h}_{j,2}^s, \dots, \mathbf{h}_{j,K_j}^s]$ . The relationship between the received signal and the transmitted signal is expressed in (2).

$$y_{j,k} = \sum_s (\mathbf{h}_{j,k}^s)^H \mathbf{x}_s + n_{j,k}^k. \quad (2)$$

Here,  $(\cdot)^H$  represents the complex conjugate transpose,  $n_{j,k}^k$  denotes the additive circularly symmetric complex Gaussian noise at  $U_{j,k}$  with zero mean and a covariance of  $\sigma^2$ .

In this research, it is assumed that the base station possesses imperfect channel information. More precisely, the estimated value of the communication channel vector, denoted as  $\tilde{\mathbf{h}}_{j,k}^s$ , is obtained through the process described in (3).

$$\tilde{\mathbf{h}}_{j,k}^s = \sqrt{(1 - \tau^2)} \mathbf{h}_{j,k}^s + \tau \mathbf{n}_{j,k}^s, \quad (3)$$

where  $\mathbf{h}_{j,k}^s$  and  $\mathbf{n}_{j,k}^s$  denote the true values of the communication channel vector and the independent error vector, respectively.  $\tilde{\mathbf{H}}_j^s = [\tilde{\mathbf{h}}_{j,1}^s, \tilde{\mathbf{h}}_{j,2}^s, \dots, \tilde{\mathbf{h}}_{j,K_j}^s]$  denotes the estimated channel matrix between  $s$ -th subarray in the base station and  $K_j$  user devices in the  $j$ -th subarray.

For the non-stationarity channel assumed in this paper, the communication channel vector between  $U_{j,k}$  and  $M_s$  antennas in the  $s$ -th subarray is represented by (4) and (5).

$$\mathbf{h}_{j,k}^s = \sqrt{M_s} (\Phi_{j,k}^s)^{\frac{1}{2}} \mathbf{z}_{j,k}^s \in \mathbb{C}^{M_s \times 1}, \quad (4)$$

$$\Phi_{j,k}^s = (\mathbf{D}_{j,k}^s)^{\frac{1}{2}} \mathbf{R}_{j,k}^s (\mathbf{D}_{j,k}^s)^{\frac{1}{2}} \in \mathbb{C}^{M_s \times M_s}, \quad (5)$$

where  $\mathbf{z}_{j,k}^s \in \mathbb{C}^{M_s \times 1}$  follows a Gaussian distribution with mean zero and covariance  $\frac{1}{M_s} \mathbf{I}_{M_s}$ ,  $\mathbf{I}_{M_s}$  denotes the identity matrix of order  $M_s$ ,  $\mathbf{R}_{j,k}^s \in \mathbb{C}^{M_s \times M_s}$  denotes the spatial correlation matrix between  $U_{j,k}$  and  $s$ -th subarray in the base station, and  $\mathbf{D}_{j,k}^s \in \mathbb{C}^{M_s \times M_s}$  denotes a diagonal matrix and has  $D_{j,k}^s$  non-zero diagonal elements between  $U_{j,k}$  and  $s$ -th subarray in the base station.

### 2.2 Precoding in RZF method

Precoding refers to the process in which signal processing is applied to the transmitted signal at the transmitter side in order to increase the signal gain at the receiver. Precoding is closely related to signal detection

processing, and the selection of precoding depends on the detection method being employed. Here, we will explain the precoding technique when using the regularized zero-forcing (RZF) method as the signal detection approach, [23].

The information vector expected to be transmitted from the  $j$ -th subarray is represented as  $\mathbf{s}_j = [s_{j,1}, s_{j,2}, \dots, s_{j,K_j}]^T$ , where  $s_{j,k}$  denotes the information transmitted from the  $j$ -th subarray to  $U_{j,k}$ . Note that  $s_{j,k}$  follows a Gaussian distribution with mean 0 and covariance  $p_{j,k}$ . The transmitted signal vector  $\mathbf{x}_j$  is generated as (6).

$$\mathbf{x}_j = \sum_{k=1}^{K_j} \mathbf{g}_{j,k} s_{j,k} = \mathbf{G}_j \mathbf{s}_j, \quad (6)$$

where  $\mathbf{G}_j = [\mathbf{g}_{j,1}, \mathbf{g}_{j,2}, \dots, \mathbf{g}_{j,K_j}]$  is the precoding matrix for user devices in the  $j$ -th subarray, and  $\mathbf{g}_{j,k}$  represents the precoding vector for  $U_{j,k}$ .  $\mathbf{g}_{j,k}$  satisfies the condition  $\|\mathbf{g}_{j,k}\|^2 = 1$ . Now, (2) is transformed into (7).

$$y_{j,k} = (\mathbf{h}_{j,k}^j)^H \mathbf{g}_{j,k} s_{j,k} + \sum_{i=1, i \neq k}^{K_j} (\mathbf{h}_{j,i}^j)^H \mathbf{g}_{j,i} s_{j,i} + \sum_{s=1, s \neq j}^S \sum_{i=1}^{K_i} (\mathbf{h}_{s,i}^s)^H \mathbf{g}_{s,i} s_{s,i} + n_{j,k}, \quad (7)$$

The first term in (7) is a desired signal, the second one is intra-subarray interference, and the third one is inter-subarray interference. One of the linear precoding schemes is RZF, [13], whose precoding matrix  $\mathbf{G}_j^{RZF}$  is denoted by (8).

$$\begin{aligned} \mathbf{F}_j &= \mathbf{H}_j^j ((\mathbf{H}_j^j)^H \mathbf{H}_j^j + \xi \mathbf{I}_{K_j})^{-1}, \\ \mathbf{G}_j^{RZF} &= \sqrt{P / \text{Tr}(\mathbf{F}_j^H \mathbf{F}_j)} \cdot \mathbf{F}_j, \end{aligned} \quad (8)$$

where  $\xi = \frac{\sigma^2}{P}$ ,  $P$  denotes average signal power, and  $\text{Tr}(\cdot)$  denotes the trace operator.

While the ZF method carries the risk of amplifying the noise component, the RZF method mitigates this issue by incorporating a regularization term  $\xi$  into the equation to prevent noise enhancement. However, the inverse operator of matrix to obtain  $\mathbf{F}_j$  makes RZF method unpractical for extremely massive MIMO systems.

### 3 Methods

Although the RZF method can cancel the interference between users and avoid noise enhanced, it requires a large complexity for inverse operation. Therefore, iterative methods have been proposed to obtain approximate solutions. In this chapter, various approaches based on the Kaczmarz Algorithm (KA) are shown, and the proposed improvements in this paper will be explained.

#### 3.1 Kaczmarz Algorithm

The KA is an iterative algorithm to solve the linear equation systems represented as  $\mathbf{A}\mathbf{x} = \mathbf{b}$ . The equation can be considered as a set of  $m$  linear equations  $\mathbf{a}_i \mathbf{x} = b_i$  for  $i = 1, 2, \dots, m$  where  $\mathbf{a}_i$  and  $b_i$  denote  $i$ -th row of  $\mathbf{A}$  and  $\mathbf{b}$ , respectively. The algorithm updates the approximation of  $\mathbf{x}$  with  $i$ -th row of  $\mathbf{A}$  and  $\mathbf{b}$  as shown in (9).

$$\mathbf{x}^{k+1} = \mathbf{x}^k + \frac{b_i - \langle \mathbf{a}_i, \mathbf{x}^k \rangle}{\|\mathbf{a}_i\|^2} \bar{\mathbf{a}}_i, \quad (9)$$

where  $i = k \bmod m$ ,  $\mathbf{x}^k$  denotes  $k$ -th approximation of  $\mathbf{x}$ ,  $\langle \cdot \rangle$  denotes inner product operation.  $\bar{\mathbf{a}}_i$  denotes complex conjugation of  $\mathbf{a}_i$ .

#### 3.2 Randomized Kaczmarz Algorithm

In order to meet the overdetermined linear systems, the randomized KA (rKA) was proposed, [16]. The difference between KA and rKA is the method of selecting row for the update of  $\mathbf{x}^k$ . The rKA selects randomly based on probability proportional to  $\|\mathbf{a}_i\|^2$  while the KA selects in order from the first row. Specifically, in rKA, the probabilities of selecting  $i$ -th row from  $m$  rows are  $\frac{1}{m}$ .

#### 3.3 RKA for RZF Precoding

In RZF precoding process, the matrix  $\mathbf{G}_j^{RZF}$  is needed to calculate. For that,  $K_j$  rKA processes are run to solve a set of linear equations as shown in (10), [22].

$$(\mathbf{A}_j)^H \mathbf{z}_j = \mathbf{s}_j, \quad (10)$$

where  $\mathbf{A}_j = [\mathbf{H}_j^j; \sqrt{\xi} \mathbf{I}_{K_j}] \in \mathbb{C}^{(M_j+K_j) \times K_j}$ .  $K_j$  processes of rKA to solve (10) are run in parallel. Specifically, the procedure of rKA for RZF precoding is shown in Algorithm 1.

---

#### Algorithm 1 rKA for RZF precoding

---

- 1: Input  $n$ -th canonical basis  $\mathbf{e}_k \in \mathbb{C}^{K_j}$  as  $\mathbf{s}_j$  for  $k$ -th process.
  - 2: Assume the solution of (10)  $\mathbf{z}_j = [\mathbf{m}_j \in \mathbb{C}^{M_j \times 1}; \sqrt{\xi} \mathbf{n}_j \in \mathbb{C}^{K_j \times 1}]$ .
  - 3: Update the approximation of  $\mathbf{z}_j$  with iterations of (9). The  $i$ -th row in (9) is selected with the probability  $P_{j,i}^{rKA} = 1/K_j$ .
  - 4: Divide last  $K_j$  components of  $\mathbf{z}_j$  obtained in  $k$ -th process by  $\xi$  and denote it as  $\mathbf{w}_{j,k}$ .
  - 5:  $\mathbf{G}_j^{RZF} = \beta \mathbf{H}_j^j \mathbf{W}_j$  is obtained where  $\mathbf{W}_j = [\mathbf{w}_{j,1}, \mathbf{w}_{j,2}, \dots, \mathbf{w}_{j,K_j}] \in \mathbb{C}^{K_j \times K_j}$ .
-

### 3.4 Sampling without Replacement rKA for RZF

The Sampling without replacement rKA, [22], referred to as SwoR-rKA, is a method in which the probability of row selection differs from the original rKA. SwoR-rKA can improve the convergence speed and spectral efficiency compared to the original. The probability of selecting  $i$ -th row in Algorithm 1 is changed into (11).

$$P_{j,i}^{SwoR} = \frac{\|\mathbf{h}_{ji}^j\|^2 + \xi}{\|\mathbf{H}_j^j\|_F^2 + K_j\xi}, \quad (11)$$

where  $\|\cdot\|_F$  denotes Frobenius norm.

In SwoR-rKA, the row is selected based on the channel quality, so SwoR-rKA intends to select the row corresponding to the user in good communication channel. This approach can allocate more resources to users in better channel than the others and that leads to enhanced SE and faster convergence speed compared to the original rKA.

### 3.5 Reverse Policy of SwoR-rKA for RZF

In SwoR-rKA, the selection of row is based on the channel condition. The row corresponding to good channel is likely to be selected. However, this approach leads to that only a limited set of linear equations can be solved well because approximation corresponding to worse channel is hardly solved due to small number of updates.

When the channel conditions are favorable, there is no need to allocate a significant computational load to the estimation process. Conversely, when the channel conditions are poor, a larger computational load is required. Therefore, the reverse policy of SwoR-rKA, referred to as RSwoR-rKA, was proposed, [24], in which the probability shown as (12) is used to select  $i$ -th row in Algorithm 1.

$$P_{j,i}^{RSwoR} = 1 - \frac{\|\mathbf{h}_{ji}^j\|^2 + \xi}{\|\mathbf{H}_j^j\|_F^2 + K_j\xi}. \quad (12)$$

(12) means that the columns corresponding to worse channel are tends to be selected.

### 3.6 Proposed Method: D'Hondt method in rKA for RZF

In Algorithm 1, it is believed that the estimation values can converge more quickly if the  $i$ -th row to be updated is appropriately selected. Therefore, we focused on the candidate selection system used in elections.

The D'Hondt system is one of the methods used to determine the allocation of seats in an election. In this system, voters cast their votes for choices such as political parties or candidates, and seats are allocated based on the election results.

The specific procedure involves voters first casting their votes for the choices, and the number of favorable votes obtained by each choice (political party or candidate) is aggregated.

Then, the determination of seat allocation takes place. Following the algorithm 2, the allocation of seats is repeated until the remaining number of seats reaches zero.

---

#### Algorithm 2 The original D'Hondt method

---

- 1: Let  $V(i)$  represent the number of votes obtained by political party  $i$  ( $i = 1, 2, \dots$ ), and  $W(i)$  represent the number of seats obtained by the party at the current stage. The number of seats to be allocated is denoted as  $S$ .
  - 2: Calculate  $V(i)/(W(i) + 1)$  for each political party and find the party  $j$  with the highest value.
  - 3: Increment  $W(i)$  by one and decrease  $S$  by one.
  - 4: Go back 2.
- 

In the D'Hondt method, the allocation of seats is carried out in order of the highest number of favorable votes. In other words, choices that have received greater support from voters are given priority in obtaining seats. This system is widely utilized as a method for determining seat allocation in elections in many countries and regions, as it allows for a direct and fair reflection of the election results.

We apply the D'Hondt method into the selection of  $i$ -th row in Algorithm 1, we call the method as D-rKA. Specifically, D-rKA select rows by Algorithm 3:

---

#### Algorithm 3 Select rows with the D'Hondt method

---

- 1: Calculate  $P_{j,i}^{RSwoR}$  for  $i = 1, 2, \dots, K_j$ .
  - 2: Vote for each row probabilistically according to  $P_{j,i}^{RSwoR}$ .
  - 3: Select row by D'Hondt method according to the number of votes.
- 

D'Hondt method try keeping the average number of votes per seat equally, so the number of updates with each row in D-rKA are more stable than the probabilistic selection method such as SwoR-rKA.

## 4 Simulation

We conducted some simulation whose aims are to confirm the changes of the BER performance with the normalized transmit powers and with the number of iterations in rKA method.

### 4.1 Parameters

The environment of developing the simulation programs is shown in Table 1. The source code of this simulation was written with Python.

The simulation program in this section used the fixed parameters and precoding methods shown in Table 2. Other parameters are described in the comments of each figure.

**Table 1:** Softwares and libraries to conduct the simulation.

Software/Library	Version
Python	3.10.6
NumPy	1.24.3
SciPy	1.10.1
Matplotlib	3.7.1

**Table 2:** Parameters used in the simulation

Parameter	Value	Explanation
$K_j$	16	The number of users in a subarray.
$M$	256	The number of antennas at base station.
$S$	16	The number of subarrays.
$M_j$	16	The number of antennas in a subarray.
$T$	16	The length of timeslot to keep channel unchanged.
m	64QAM	Digital modulation method.
trials	$10^5$	The number of trials with fixed channel states.
$\tau$	0.3	The quality of channel state information at base station.
$\sigma^2$	1 dBm	The power of noise.

### 4.2 Results

We show the results in two viewpoints.

- The BER performances against the normalized transmit power (NTP) with fixed number of iterations in rKA algorithm.
- The BER performances against the number of iterations in rKA algorithm with fixed NTP.

#### 4.2.1 BER performance against NTP

The rKA method is an iterative method, so the number of iterations is important to make the accuracy of approximation higher. However, too many iterations are wasteful because residuals remain. Therefore, we

conducted the simulation that compare the BER performance against the number of iterations. The results are shown in Figure 1, Figure 2, Figure 3, Figure 4, Figure 5, Figure 6, and Figure 7. The horizontal line in each figure indicates the normalized transmit power and vertical one indicates the BER performances. The number of iterations in rKA process are 20, 40, 60, 80, 100, 120, and 140, respectively. The channels in all simulations are non-stationary and the base stations in all simulations have imperfect channel state information.

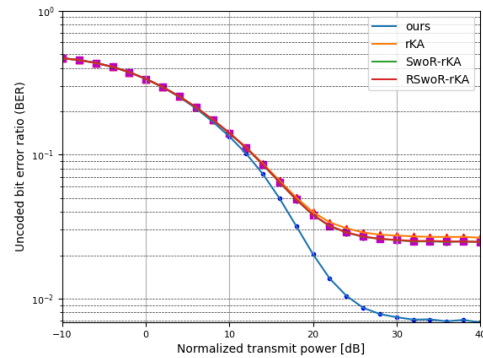


**Figure 1:** BER performances against normalized transmit power with 20 times iterations in rKA algorithm. The channel is non-stationary one and the base stations have imperfect channel state information.

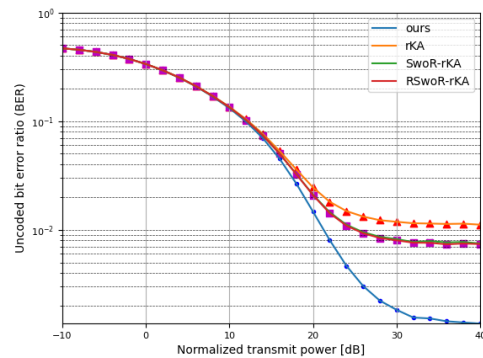


**Figure 2:** BER performances against normalized transmit power with 40 times iterations in rKA algorithm. The channel is non-stationary one and the base stations have imperfect channel state information.

#### 4.2.2 BER performance against the number of iterations

Next, we compare the results of Figure 1, Figure 2, Figure 3, Figure 4, Figure 5, Figure 6, and Figure 7, according to changes in the number of iterations. The results are shown in Figure 8, Figure 9, and Figure 10.

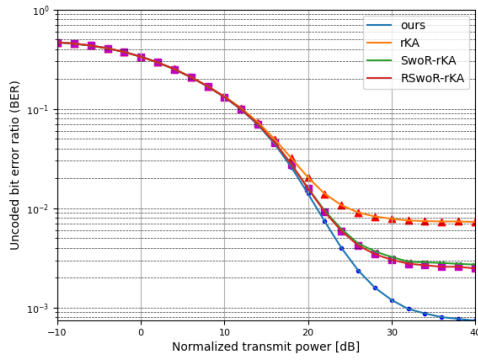


**Figure 3:** BER performances against normalized transmit power with 60 times iterations in rKA algorithm. The channel is non-stationary one and the base stations have imperfect channel state information.

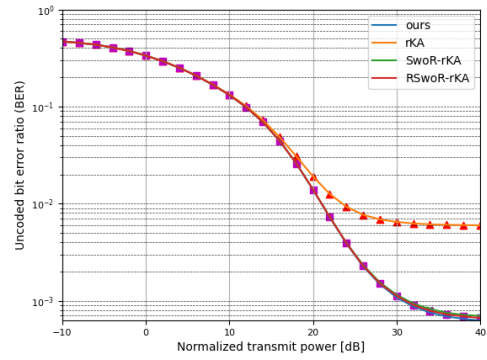


**Figure 6:** BER performances against normalized transmit power with 120 times iterations in rKA algorithm. The channel is non-stationary one and the base stations have imperfect channel state information.

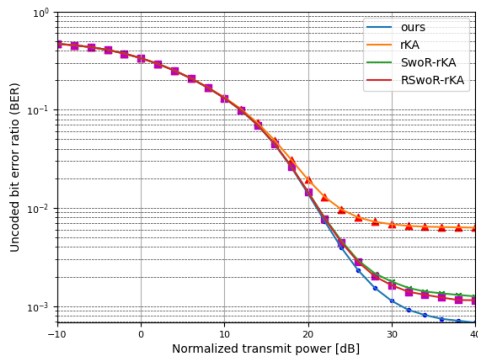


**Figure 4:** BER performances against normalized transmit power with 80 times iterations in rKA algorithm. The channel is non-stationary one and the base stations have imperfect channel state information.

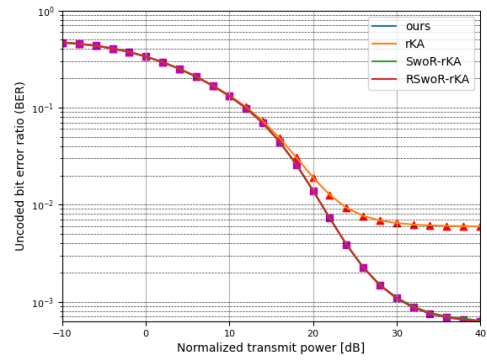


**Figure 7:** BER performances against normalized transmit power with 140 times iterations in rKA algorithm. The channel is non-stationary one and the base stations have imperfect channel state information.

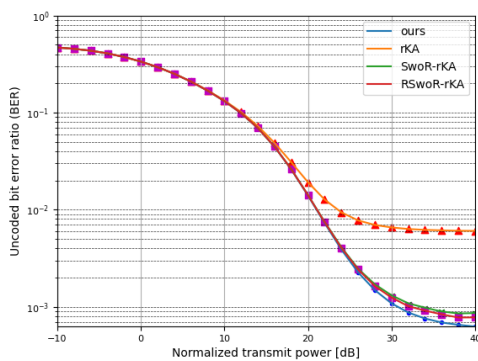


**Figure 5:** BER performances against normalized transmit power with 100 times iterations in rKA algorithm. The channel is non-stationary one and the base stations have imperfect channel state information.

These figures illustrate the BER performance at NTP values of 20, 30, and 40, respectively. The horizontal line in each figure indicates the number of iterations in rKA algorithm and vertical one indicates the BER performances.

### 4.3 Consideration

As illustrated in Figure 1, Figure 2, Figure 3, Figure 4, Figure 5, Figure 6, and Figure 7, our method shows significantly better BER performance with a small number of iterations, especially when the normalized transmit power (NTP) exceeds approximately 10 dB. This result suggests that our method achieves a more accurate approximation with fewer iterations compared to other methods. The difference between the methods becomes smaller as the number of iterations increases, but even at lower NTPs and higher iteration counts, our method continues to outperform the others.

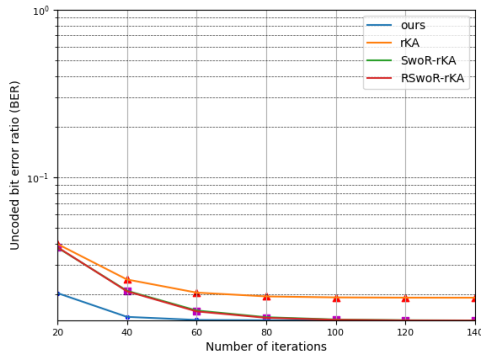


**Figure 8:** BER performances against the number of iteration in rKA algorithm. NTP is 20 dB and the channel is non-stationary one. The base stations have imperfect channel state information.

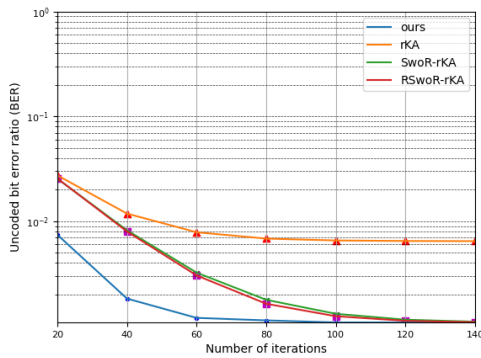


**Figure 9:** BER performances against the number of iteration in rKA algorithm. NTP is 30 dB and the channel is non-stationary one. The base stations have imperfect channel state information.

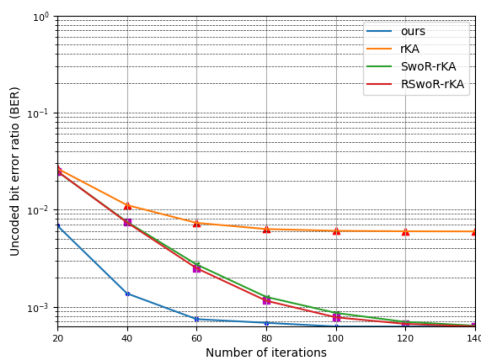


**Figure 10:** BER performances against the number of iteration in rKA algorithm. NTP is 40 dB and the channel is non-stationary one. The base stations have imperfect channel state information.

One of the key findings, as seen in Figure 8, Figure 9, and Figure 10, is that our method maintains a superior BER performance, particularly with fewer iterations. In extremely massive MIMO systems, where a large number of antennas is employed, reducing the number of iterations is critical to minimizing computational complexity. The results demonstrate that our method is effective in achieving low BER while significantly reducing the required number of iterations. For instance, at 20, 30, and 40 dB NTP, our method converges to a lower BER than the other methods even with fewer iterations.

In practical applications, the reduced number of iterations has important implications. It can lead to faster processing times and lower energy consumption in real-time communication systems. Massive MIMO systems, particularly in future 6G networks, will require efficient algorithms to handle the increased computational demands. The ability of our method to achieve better BER with fewer iterations makes it highly suitable for such large-scale systems.

However, despite the clear advantages, some limitations remain. While our method performs well at higher NTPs, residual errors limit its performance at very high transmit powers. Exploring how the method performs under different channel conditions, such as those with more severe non-stationarity or interference, would also be valuable.

## 5 Conclusion

The proposed method, which innovatively applies the D'Hondt method for row selection in the randomized Kaczmarz algorithm, stands out by offering faster convergence and better BER performance. Unlike conventional methods that rely on probabilistic selection, our approach ensures a more balanced and efficient update process, making it particularly advantageous in scenarios with high normalized transmit power.

Our simulation results demonstrated that our proposed method significantly improves BER performance compared to existing rKA-based methods, particularly in scenarios with imperfect channel state information at the base stations. The ability to achieve better BER with fewer iterations highlights the computational efficiency of our method, making it a suitable solution for real-world applications in massive MIMO systems, where reducing complexity is crucial.

The main contribution of this research is the innovative application of the D'Hondt method, which helps balance the update process in rKA, leading to more stable and accurate results. This approach is particularly useful in large-scale systems where computational efficiency is key.

With these findings, we recommend that the proposed method be implemented in large-scale wireless communication systems, such as future 6G networks, where the reduction of computational complexity in precoding is critical. The faster convergence and improved BER performance, especially at higher normalized transmit powers, make our method well-suited for real-time applications requiring high reliability and low latency. Additionally, the proposed method could be further optimized for hardware implementation, allowing for even faster processing in practical systems.

For future work, we plan to address the residual errors that limit the performance of our method at very high transmit powers. Moreover, testing the method in real-world hardware environments will be essential to ensure that the computational savings translate into tangible performance improvements. Investigating the performance of our method under different channel conditions, such as perfect channel state information or more severe non-stationary environments, will play an essential role in further validating and enhancing the robustness of the method.

#### References:

- [1] S. W. Nourildean, M. D. Hassib, and Y. A. Mohammed, "Internet of Things Based Wireless Sensor Network: A Review," *Indonesian Journal of Electrical Engineering and Computer Science*, vol.27, no.1, pp.246-261, 2022.
- [2] M. Vaezi et al., "Cellular, Wide-Area, and Non-Terrestrial IoT: A Survey on 5G Advances and the Road Toward 6G," *IEEE Communications Surveys & Tutorials*, vol.24, no.2, pp.1117-1174, 2022.
- [3] L. Chettri and R. Bera, "A Comprehensive Survey on Internet of Things Toward 5G Wireless Systems," *IEEE Internet of Things Journal*, vol.7, no.1, pp.16-32, 2020.
- [4] K. Shafique, B. A. Khawaja, F. Sabir, S. Qazi, and M. Mustaqim, "Internet of Things for Next-Generation Smart Systems: A Review of Current Challenges, Future Trends and Prospects for Emerging 5G-IoT Scenarios," *IEEE Access*, vol.8, pp.23022-23040, 2020.
- [5] L. Lu, G. Y. Li, A. L. Swindlehurst, A. Ashikhmin, and R. Zhang, "An Overview of Massive MIMO: Benefits and Challenges," *IEEE Journal of Selected Topics in Signal Processing*, vol.8, no.5, pp.742-758, 2014.
- [6] S. Suverna and P. K. Malik, "A Comprehensive Survey of Massive MIMO Based on 5G Antennas," *International Journal of RF and Microwave Computer-Aided Engineering*, vol.32, no.12, 2022.
- [7] T. Fukuda, "Improvement in Accuracy of Signal Detection Aided by Element-Based Lattice Reduction for Massive MIMO Wireless Communication Systems," *Research Report of Kitakyushu National College of Technology*, vol.52, pp.23-27, 2019.
- [8] T. Fukuda, S. Uchimura, K. Fukai, and H. A. Zhao, "An Improved Element Based Lattice Reduction Algorithm for Large MIMO Detection," in *Proc. The 6th IIAE International Conference on Intelligent Systems and Image Processing*, pp.56-61, 2018.
- [9] O. T. Demir, E. Björnson, and L. Sanguinetti, "Cell-Free Massive MIMO with Large-Scale Fading Decoding and Dynamic Cooperation Clustering," in *Proc. WSA 2021; 25th International ITG Workshop on Smart Antennas*, pp.1-6, 2021.
- [10] G. N. Reddy, C. V. Ravikumar, and A. Rajesh, "Literature Review and Research Direction Towards Channel Estimation and Hybrid Pre-coding in Mmwave Massive MIMO Communication Systems," *Journal of Reliable Intelligent Environments*, pp.1-20, 2022.
- [11] D. Verenzuela, E. Björnson, X. Wang, M. Arnold, and S. ten Brink, "Massive-MIMO Iterative Channel Estimation and Decoding in the Uplink," *IEEE Transactions on Communications*, vol.68, no.2, pp.854-870, 2020.
- [12] N. Fatema, G. Hua, Y. Xiang, D. Peng, and I. Natgunanathan, "Massive MIMO Linear Precoding: A Survey," *IEEE Systems Journal*, vol.12, no.4, pp.3920-3931, 2018.
- [13] M. A. Albreem, A. H. A. Habbash, A. M. Abu-Hudrouss, and S. S. Ikki, "Overview of Precoding Techniques for Massive MIMO," *IEEE Access*, vol.9, pp.60764-60801, 2021.
- [14] L. N. Ribeiro, S. Schwarz, and M. Haardt, "Low-Complexity Zero-Forcing Precoding for XL-MIMO Transmissions," in *Proc. EUSIPCO*, pp.1621-1625, 2021.
- [15] E. Björnson, M. Bengtsson, and B. Ottersten, "Optimal Multiuser Transmit Beamforming: A Difficult Problem with a Simple Solution Structure [Lecture Notes]," *IEEE Signal Processing Magazine*, vol.31, no.4, pp.142-148, 2014.



- [16] T. Strohmer and R. Vershynin, "A Randomized Solver for Linear Systems With Exponential Convergence," in *Approximation, Randomization, and Combinatorial Optimization. Algorithms and Techniques: 9th International Workshop on Approximation Algorithms for Combinatorial Optimization Problems, APPROX 2006 and 10th International Workshop on Randomization and Computation, RANDOM 2006*, pp.499–507, 2006.
- [17] Y. C. Eldar and D. Needell, "Acceleration of Randomized Kaczmarz Method via the Johnson–Lindenstrauss Lemma," *Numerical Algorithms*, vol.58, no.2, pp.163–177, 2011.
- [18] Z. Wang, J. Zhang, H. Q. Ngo, B. Ai, and M. Debbah, "Uplink Precoding Design for Cell-Free Massive MIMO With Iteratively Weighted MMSE," *IEEE Transactions on Communications*, vol.71, no.3, pp.1646–1664, 2023.
- [19] Z. Feng et al., "A Precoding Scheme for Polar Coded Uplink MU-MIMO Systems," in *Proc. ICC 2022 - IEEE International Conference on Communications*, Seoul, Korea, Republic of, 2022, pp.2489–2494, 2022.
- [20] A. Boukharouba, M. Dehemchi, and A. Bouhafer, "Low-Complexity Signal Detection and Precoding Algorithms for Multiuser Massive MIMO Systems," *SN Applied Science*, vol.3, no.169, 2021.
- [21] M. N. Boroujerdi, S. Haghghatshoar, and G. Caire, "Low-Complexity Statistically Robust Precoder/Detector Computation for Massive MIMO Systems," *IEEE Trans. Wireless Commun.*, vol.17, no.10, pp.6516–6530, 2018.
- [22] B. Xu, Z. Wang, H. Xiao, J. Zhang, B. Ai, and D. W. K. Ng, "Low-Complexity Precoding for Extremely Large-Scale MIMO Over Non-Stationary Channels," in *Proc. IEEE International Conference on Communications (ICC)*, 2023.
- [23] J. Zhang, J. Zhang, E. Björnson, and B. Ai, "Local Partial Zero-Forcing Combining for Cell-Free Massive MIMO Systems," *IEEE Trans. Commun.*, vol.69, no.12, pp.8459–8473, 2021.
- [24] T. Fukuda, "Improvement of SwoR-rKA Precoding Method for Extremely Large-Scale MIMO With the Same Computational Complexity," *International Journal of Communications*, vol.8, pp.6–14, 2023.

#### **Contribution of Individual Authors to the Creation of a Scientific Article (Ghostwriting Policy)**

The author solely contributed in the present research, at all stages from the formulation of the problem to the final findings and solution.

#### **Sources of Funding for Research Presented in a Scientific Article or Scientific Article Itself**

No funding was received for conducting this study.

#### **Conflicts of Interest**

The author is affiliated with Shimonoseki City University, a public university corporation located in Shimonoseki City, which is the subject of this research.

#### **Creative Commons Attribution License 4.0 (Attribution 4.0 International, CC BY 4.0)**

This article is published under the terms of the Creative Commons Attribution License 4.0

[https://creativecommons.org/licenses/by/4.0/deed.en\\_US](https://creativecommons.org/licenses/by/4.0/deed.en_US)